

AuPt Alloy on TiO₂: A Selective and Durable Catalyst for L-Sorbose Oxidation to 2-Keto-Gulonic Acid

Carine E. Chan-Thaw,^[a] Lidia E. Chinchilla,^[c] Sebastian Campisi,^[a] Gianluigi A. Botton,^[c] Laura Prati,^[a] Nikolaos Dimitratos,^{*[b]} and Alberto Villa^{*[a]}

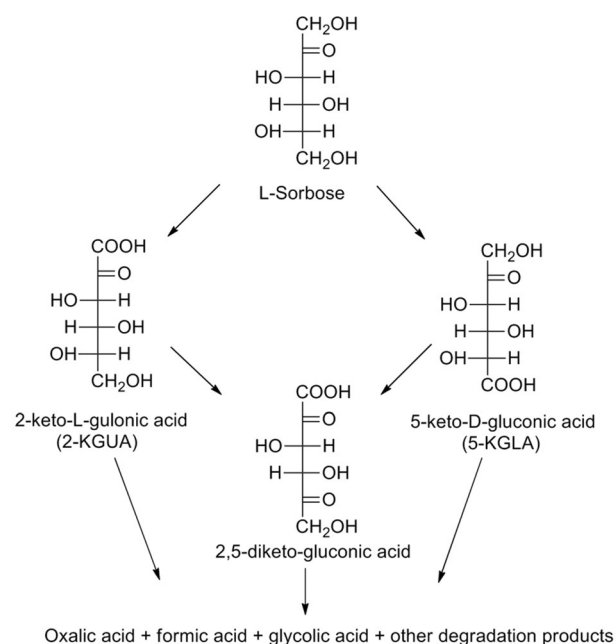
Pt nanoparticles were prepared by a sol immobilization route, deposited on supports with different acid/base properties (MgO, activated carbon, TiO₂, Al₂O₃, H-Mordenite), and tested in the selective oxidation of sorbose to 2-keto-gulonic acid (2-KGUA), an important precursor for vitamin C. In general, as the basicity of the support increased, a higher catalytic activity occurred. However, in most cases, a strong deactivation was observed. The best selectivity to 2-KGUA was observed with

acidic supports (TiO₂ and H-Mordenite) that were able to minimize the formation of C₁/C₂ products. We also demonstrated that, by alloying Pt to Au, it is possible to enhance significantly the selectivity of Pt-based catalysts. Moreover, the AuPt catalyst, unlike monometallic Pt, showed good stability in recycling because of the prevention of metal leaching during the reaction.

Introduction

Carbohydrates represent suitable and sustainable platform molecules as replacements for fossil-derived resources in the synthesis of fine chemicals.^[1–5] The selective oxidation of carbohydrates could be challenging for the production of several products.^[1–5] The liquid-phase oxidation of glucose to gluconic acid with noble metals (Pd, Pt, and Au) and molecular oxygen as the oxidant has been the subject of several investigations.^[2,4,6] By contrast, only a few studies have been reported with regard to the catalytic oxidation of L-sorbose to 2-keto-gulonic acid (2-KGUA), an intermediate in the production of L-ascorbic acid (vitamin C).^[7–13] Presently, the transformation of L-sorbose to 2-KGUA consists of an expensive and time-consuming three-step process that involves the protection of sorbose with acetone, oxidation with NaOCl or KMnO₄, and hydrolytic deprotection to give 2-KGUA.^[14] Efforts have been made to replace this methodology with a more convenient catalytic route consisting of a single-step process in the presence of noble-metal-based catalysts and molecular oxygen as the oxidant in

aqueous solution.^[7–13] Platinum-based catalysts were more active and more selective for 2-KGUA than palladium-based ones.^[7–13] Moreover, a variety of products deriving from parallel or consecutive reactions has been reported to occur, as shown in Scheme 1. In particular, the oxidation of the OH group on



Scheme 1. Reaction scheme for L-sorbose oxidation.

the C6 atom instead of the one on the C1 atom leads to the formation of 5-keto-gluconic acid (5-KGLA) instead of 2-KGUA (Scheme 1), with both reactions showing a similar rate. Moreover, products deriving from C–C cleavage, such as glycolic,

[a] Dr. C. E. Chan-Thaw, S. Campisi, Prof. L. Prati, Dr. A. Villa
Dipartimento di Chimica
Università degli Studi di Milano
via Golgi 19, 20133 Milano (Italy)
alberto.villa@unimi.it

[b] Dr. N. Dimitratos
Cardiff Catalysis Institute, School of Chemistry
Cardiff University
Main Building, Park Place, Cardiff, CF10 3AT (UK)
E-mail: DimitratosN@cardiff.ac.uk

[c] Dr. L. E. Chinchilla, Prof. G. A. Botton
Canadian Centre of Electron Microscopy and Department of Materials Science and Engineering
McMaster University
1280 Main Street West, Hamilton, Ontario L8S 4M1 (Canada)

Supporting Information for this article is available on the WWW under <http://dx.doi.org/10.1002/cssc.201501202>.

oxalic, and formic acids, are formed, particularly if high-temperature and alkaline conditions are used.^[7–13]

Brönnimann et al., by using Pd/Al₂O₃, reported a selectivity of 67% at 58% conversion at a moderate temperature (50 °C) and a pH value close to neutrality (7.3).^[7] In this study, a high metal/substrate molar ratio (1:30) was used as a result of the low pH value required for the stability of the desired product. It has been shown, indeed, that the presence of a base accelerates H abstraction, which is the rate-determining step in alcohol oxidation.^[11] Moreover, a strong deactivation phenomenon occurred, mainly because of Pt passivation by O₂ and the irreversible adsorption of products.^[7] The same group showed that the addition of Bi or Pb to Pt increased the reaction rate but decreased the selectivity for 2-KGUA (31–38%, instead of 67% with unmodified Pt).^[7] By contrast, the modification of Pt with phosphines or amines could significantly enhance the selectivity but slightly decreased the activity and the catalyst durability.^[8–11] The best reported results were achieved with hexamethylenetetramine with a selectivity of 80% for 2-KGUA at 50% conversion.^[10] Subsequently, it has been reported that Pt impregnated on a resin, such as hyper-cross-linked polystyrene, is able to produce 2-KGUA with a selectivity of 98% and full conversion at *T* = 70 °C and pH 6.5.^[12,13]

However, these latter results have recently been under debate because of the reliability of using the iodometric method to determine the yield of 2-KGUA.^[15] It is therefore evident that the development of a selective and durable catalyst for L-sorbose oxidation to 2-KGUA still remains a challenge.

It was reported that, by alloying Au with Pt, it is possible to enhance the activity, selectivity, and stability of Pt catalysts in the liquid-phase oxidation of glycerol and sorbitol, even in the absence of a base.^[16–18] The addition of Au has been shown to improve the resistance of Pt to overoxidation by O₂ and to avoid or minimize the leaching of metals into the reaction solution.^[1,16–19] Furthermore, it was highlighted that the support can also play a fundamental role in improving the selectivity, by limiting the occurrence of side reactions.^[16] The aim of this work is to explore the extension of the use of alloyed AuPt catalysts in the liquid-phase oxidation of L-sorbose and to determine if the use of these alloyed catalysts can also be beneficial in this case in terms of activity, selectivity, and stability. In addition, the role of the support on the catalytic performance was investigated by depositing the metal nanoparticles (NPs) on supports with different morphologies and surface chemistries, namely H-Mordenite, TiO₂, activated carbon, and MgO.^[16,18]

Results and Discussion

Pt catalysts were synthesized with a sol immobilization technique.^[20] Pt nanoparticles with a mean diameter of 3.2 nm (Table S1 in the Supporting Information) were synthesized in the presence of polyvinyl alcohol (PVA) as the protective agent and NaBH₄ as the reducing agent. The Pt NPs were then immobilized on the different metal oxides (H-Mordenite, TiO₂, Al₂O₃, MgO) or on activated carbon (AC). A small increase of the particle size was observed for Pt nanoparticles after the immobilization on the support, in particular for Pt/Al₂O₃, for which a Pt

mean diameter of 4.4 nm was measured (Table S1 in the Supporting Information). The catalytic performances of the supported nanoparticles were tested in the L-sorbose oxidation by using a Metrohm Titrino 718 apparatus with the ability to provide high precision control of the pH value (± 0.01) and a glass reactor that was especially designed to perform reactions under pressure (maximum pressure of 4 bar) and controlled pH values (Scheme S1 in the Supporting Information). The reaction conditions were optimized to maximize the yield of 2-KGUA (0.3 M sorbose, pressure of O₂ = 2 bar, *T* = 50 °C, metal/sorbose = 1:250 (mol/mol), pH 7.5).

The catalytic data are presented in Table 1. As all of the Pt catalysts showed similar mean diameter (3–4 nm; Table S1 in the Supporting Information), the different activities can be likely addressed to the different surface chemistries of the sup-

Table 1. Results of sorbose oxidation with Pt, Au, and AuPt catalysts at 30% conversion and after 8 h of reaction time.^[a]

Catalyst	Conversion [%]	Selectivity [%]				Carbon balance [%]
		2-KGUA	5-KGLA	C ₁ /C ₂	others	
1%Pt/MgO	30	24	7	50	4	85
	81 ^[b]	8	5	54	6	73
1%Pt/Al ₂ O ₃	30	38	12	35	8	96
	37 ^[b]	36	12	37	8	96
1%Pt/AC	30	44	10	43	7	98
	59 ^[b]	40	8	46	8	95
1%Pt/TiO ₂	30	59	14	20	5	98
	51 ^[b]	57	15	21	5	98
1%Pt/H-Mordenite	30	48	12	24	12	96
	29 ^[b]	48	12	24	12	96
1%AuPt/AC	30	58	18	19	3	98
	89 ^[b]	54	15	26	3	98
1%AuPt/TiO ₂	30	80	11	4	4	99
	83 ^[b]	75	10	9	5	99

[a] Reaction conditions: 0.3 M Sorbose, O₂ pressure = 2 bar, *T* = 50 °C, metal/sorbose = 1:250 mol/mol, pH 7.5. [b] Conversion after 8 h of reaction time.

port and possible metal–support interactions. We found a direct correlation between the activity and the acid/base properties of the support. In general, with an increase in the basicity of the support (MgO (pH 12.1) > Al₂O₃ (8.1) ≥ AC (7.6) > TiO₂ (5.5) > H-Mordenite (2.8); Table S2 in the Supporting Information), a higher catalytic activity was observed: Pt/MgO (81%) > Pt/AC (59%) > Pt/TiO₂ (51%) > Pt/Al₂O₃ (37%) > Pt/H-Mordenite (29%; Table 1) after 8 h of reaction time.

This trend confirms the observation that a basic support is able to accelerate the H abstraction, which is the rate-determining step in the oxidative dehydrogenation of alcohols and polyols.^[1] Pt/Al₂O₃ represents an exception by showing an activity that is lower than that of more acidic catalysts. We ascribed this behavior to the bigger Pt particle size (4.4 nm) relative to that of the other catalysts (3.4–3.7 nm). For a correct comparison, the selectivity was first evaluated at iso conversion (30%; Table 1). In terms of selectivity, Pt/MgO, the most active catalyst, showed a very low selectivity for 2-KGUA (24% at 30% conversion) with the promotion of the formation of C₁

and C₂ products derived from C–C cleavage. Indeed, at higher conversion (81%), the formation of degradation products is more evident and a selectivity of only 8% was obtained (Table 1). Moreover, the carbon balance of around only 85% was ascribed to the formation of CO₂. Pt NPs supported on slight basic catalysts (Al₂O₃ and AC) showed a higher selectivity to 2-KGUA (38 and 44%, respectively) with a limited formation of liquid C₁/C₂ products and CO₂ relative to Pt/MgO (Table 1). The best selectivity was observed with acidic supports (TiO₂ and H-Mordenite) that were able to minimize the formation of C₁/C₂ products. Pt/TiO₂ showed the best results with a selectivity for 2-KGUA of 59% (Table 1). The selectivity did not significantly change at higher conversion (Table 1 and Figure S1 a in the Supporting Information).

From an examination of the reaction profiles (Figure S2 in the Supporting Information), it can be observed that the majority of the catalysts, except Pt/MgO, did not show good durability, as evidenced by a strong deactivation phenomenon after 4 h of reaction time. This deactivation could be explained by an irreversible chemisorption of the carboxylic acids on the Pt active sites. Moreover, inductively coupled plasma (ICP) analysis showed a moderate Pt leaching (2–6%).

To improve the catalyst durability, we modified the Pt catalysts by adding Au, in a nominal ratio of Au:Pt=6:4, and selected the Pt/TiO₂ and Pt/AC catalysts that showed the highest selectivity for 2-KGUA. AuPt catalysts were prepared by a two-step procedure, in which the Pt PVA-protected salt was slowly reduced by H₂ in presence of supported Au. A similar mean diameter for the AuPt nanoparticles (3.4–3.7 nm) was obtained in both cases. The detailed morphology of AuPt/AC is reported elsewhere^[19] and reveals the presence of AuPt alloy, whereas a full characterization of AuPt/TiO₂ is described herein.

High-angle annular dark-field (HAADF) images of the AuPt/TiO₂ catalyst showed well-dispersed metal nanoparticles on TiO₂ (Figure S3 a,b in the Supporting Information). The catalyst had a normal distribution of particles with sizes in the 1–7 nm range, with a mean diameter of (3.7 ± 0.1) nm and a total metal dispersion of around 30% (Table S1 and Figure S4 in the Supporting Information). Individual atoms and sub-nanometer clusters were also detected in the catalyst, along with a limited number of larger agglomerated structures (Figure S3 c,d in the Supporting Information).

A representative selection of HAADF scanning transmission electron microscopy (STEM) images of the AuPt particles supported on TiO₂ and the corresponding energy-dispersive X-ray spectroscopy (XEDS) elemental maps are presented in Figure 1. The spatial distribution of Au and Pt shown in Figure 1 revealed the coexistence of Pt and Au elements within the nanoparticle, which suggests the formation of random gold–platinum alloy structures. Quantitative XEDS analysis was performed in about 26 nanoparticles. The resulting particle-size-composition diagram showed the presence of very small platinum nanoparticles (around 3.5 nm), gold nanoparticles varying between 3 and 9 nm in size, and bimetallic nanoparticles in the composition range of 35–65 wt% Pt (Figure S5 in the Supporting Information). The XEDS analyses from individual particles confirmed that the majority of the supported nanoparti-

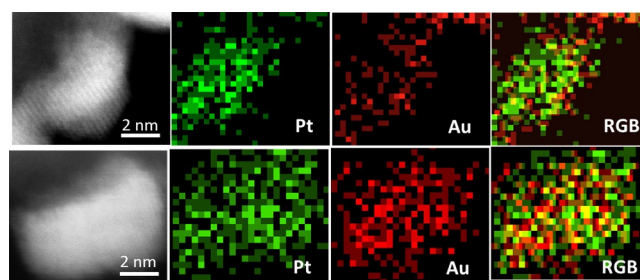


Figure 1. HAADF STEM images of the AuPt/TiO₂ catalyst and the corresponding Au-L_α and Pt-L_α elemental maps from individual particles.

cles were bimetallic (AuPt) in nature. A high-magnification HAADF STEM image and the corresponding XEDS spectrum from a representative AuPt/TiO₂ particle that demonstrates the AuPt alloy structure is shown in Figure 2.

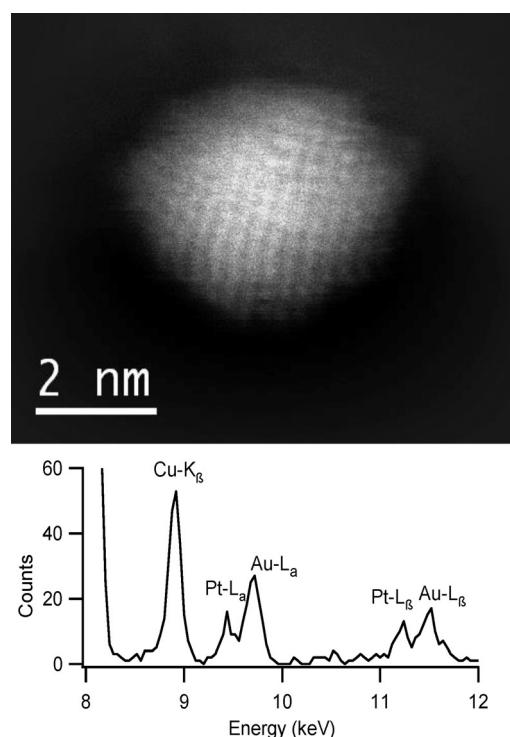


Figure 2. Representative high-magnification HAADF STEM image of the AuPt/TiO₂ catalyst and the corresponding XEDS spectrum obtained from the individual nanoparticle.

The bimetallic catalysts showed an enhanced conversion relative to the corresponding monometallic counterparts (Table 1). Moreover, the presence of Au increased the durability of the catalysts. Indeed, in a comparison of the reaction profiles of Pt and AuPt catalysts (Figure 3), the bimetallic catalysts appeared less prone to deactivate during the reaction.

In terms of selectivity, AuPt catalysts showed higher selectivity for 2-KGUA than the corresponding monometallic catalysts (Table 1). At approximately 90% conversion, AuPt/AC gave a selectivity of 54% with the formation of 26% of C₁/C₂ products, whereas AuPt/TiO₂ showed a selectivity of 75%, one of the

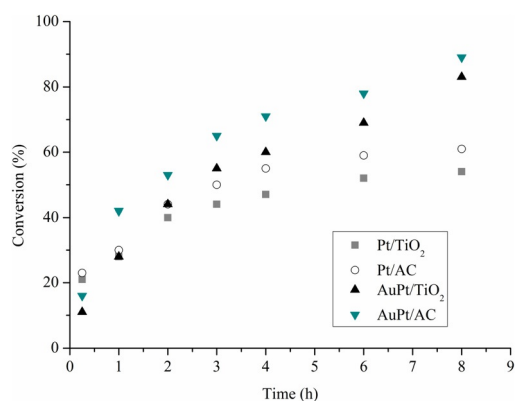


Figure 3. Reaction profiles for Pt and AuPt catalysts supported on activated carbon and TiO₂.

best reported results in the literature, and showed a significant decrease in the formation of C–C cleavage products (9%). It was reported that the C–C bond cleavage can be a result of the formation of H₂O₂ through O₂ reduction by a metal hydride.^[16,21–23] Therefore, we determined the amount of H₂O₂ present at the end of the reaction, by titration with KMnO₄. In the presence of AuPt/TiO₂, a concentration of 0.089 mmol L⁻¹ of H₂O₂ was detected, whereas a ten times higher amount of H₂O₂ was detected with AuPt/AC (0.813 mmol L⁻¹), which is directionally consistent with the selectivity data obtained. Experiments on H₂O₂ decomposition with the two catalysts showed a similar degradation rate (Figure S6 in the Supporting Information). Therefore, we ascribed the different selectivity of the two catalytic systems to the higher tendency of AuPt/AC to catalyze the reaction between H₂O₂ and sorbose, which thus promotes the C–C scission.

To evaluate the resistance of AuPt to deactivation, stability tests have been performed on AuPt/TiO₂, the catalyst presenting the highest selectivity for 2-KGUA (75%; Figure 4). Recycling experiments were performed by filtering and using the catalyst in the next run without any further purification. The catalyst was stable until the fourth run, and then a gradual loss of activity was observed. Transmission electron microscopy

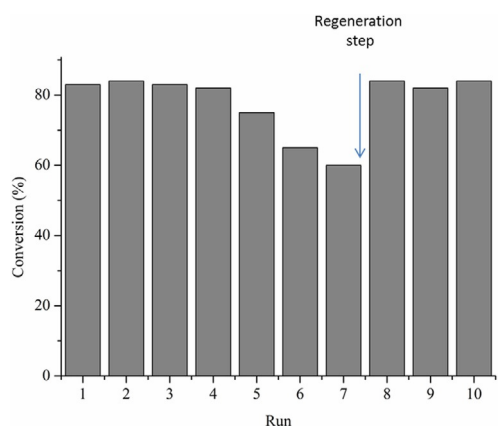


Figure 4. Results of the stability test for AuPt/TiO₂.

(TEM) performed on the used catalyst did not show any appreciable changes in AuPt particle size (Table S1 in the Supporting Information); therefore, the deactivation was attributed to the presence of adsorbed species. Indeed, after thorough washing of the catalyst with distilled water, the original activity was restored and kept at least for another two runs. No leaching of Au or Pt was observed from the ICP results, which confirmed the stability of the AuPt/TiO₂ catalyst.

Conclusions

In summary, we have demonstrated that, by alloying Pt to Au, it is possible to enhance significantly the selectivity of Pt-based catalysts in the selective oxidation of sorbose to 2-keto-gulonic acid (2-KGUA), an important precursor for vitamin C. In particular, by choosing the appropriate support (TiO₂), it is possible to increase the selectivity for 2-KGUA, probably by decreasing the reactivity of H₂O₂ with L-sorbose and 2-KGUA to form C₁/C₂ products. Moreover, the AuPt/TiO₂ catalyst showed good stability in recycling. For the restoration of the initial activity after four runs, the catalyst needs to be washed with an excess of water, probably to remove strongly adsorbed species from the active sites.

Experimental Section

Materials

NaAuCl₄·2H₂O and K₂PtCl₄ were from Aldrich (99.99% purity). H-Mordenite and TiO₂ P25 were from Degussa, Al₂O₃ from Condea, MgO from Alfa Aesar, and activated carbon (X40S; surface area = 1086 m² g⁻¹; pore volume (PV) = 1.5 mL g⁻¹, intensity ratio of the D and G bands (*I_D/I_G*) = 2.4) was from Camel. NaBH₄ (purity > 96%) from Fluka and polyvinylalcohol (PVA; *M_w* = 13 000–23 000, 87–89% hydrolyzed) from Aldrich were used. A 1 wt% PVA solution in water was prepared. The gaseous oxygen from SIAD was 99.99% pure.

Catalyst preparation

Au_{PVA}: Solid NaAuCl₄·2H₂O (0.051 mmol) and PVA (1 wt%) solution (Au/PVA = 1:0.5 w/w) were added to H₂O (100 mL). After 5 min, NaBH₄ (0.1 M) solution (Au/NaBH₄ = 1:4 mol/mol) was added to the yellow solution with vigorous magnetic stirring. Within a few minutes of sol generation, the colloid was immobilized by adding the support with vigorous stirring. The amount of support was calculated as having a total final metal loading of 1 wt%. After 2 h, the slurry was filtered, and the catalyst was washed thoroughly with distilled water (neutral mother liquors) and dried at *T* = 80 °C for 4 h.

Pt_{PVA}: Solid K₂PtCl₄ (0.051 mmol) and PVA (1 wt%) solution (Pt/PVA = 1:0.5 w/w) were added to H₂O (100 mL). After 5 min, H₂ was bubbled through (50 mL min⁻¹) under atmospheric pressure at room temperature for 2 h. The colloid was immobilized by adding the support with vigorous stirring. The amount of support was calculated as having a total final metal loading of 1 wt%. After 2 h, the slurry was filtered, and the catalyst was washed thoroughly with distilled water (neutral mother liquors) and dried at *T* = 80 °C for 4 h.

AuPt_{PVA}: NaAuCl₄·2H₂O (Au: 0.031 mmol) was dissolved in H₂O (60 mL), and PVA (1 wt%) was added (Au/PVA = 1:0.5 w/w). The yellow solution was stirred for 3 min, after which 0.1 M NaBH₄ (Au/NaBH₄ = 1:4 mol/mol) was added with vigorous magnetic stirring. Within a few minutes of sol generation, the gold sol was immobilized by adding the support with vigorous stirring. The amount of support was calculated as having a gold loading of 0.60 wt%. After 2 h, the slurry was filtered, and the catalyst was washed thoroughly with distilled water (neutral mother liquors). The Au/support was dispersed in H₂O (40 mL), with K₂PtCl₄ (Pt: 0.021 mmol) and PVA solution (Pt/PVA = 1:0.5 w/w) added. H₂ was bubbled through (50 mL min⁻¹) under atmospheric pressure at room temperature for 2 h. The slurry was filtered, and the catalyst was washed thoroughly with distilled water (neutral mother liquors) and dried at T = 80 °C for 4 h. The total metal loading was 1 wt%.

Oxidation procedure

Reactions were performed in a thermostated glass reactor (50 mL) provided with an electronically controlled magnetic stirrer connected to a large reservoir (5000 mL) containing oxygen at 3 bar. The oxygen uptake was followed by a mass flow controller connected to a computer through an analog-to-digital board, which plotted a flow-time diagram. The reactor was specially designed to measure the pH value under pressure. The pH value was automatically controlled by a Metrohm Titrino 718 apparatus and maintained by adding NaOH (0.5 M). Sorbose (0.3 M) and the catalyst (metal/sorbose = 1:250 mol/mol) were mixed in distilled water (total volume 20 mL). NaOH (0.5 M) was added until the desired pH value (7.5) was reached. The reactor was pressurized at 2 bar of N₂ and thermostated at the appropriate temperature. Once the required temperature (50 °C) was reached, the gas supply was switched to oxygen and the monitoring of the reaction was started.

Recycling tests were performed under the same experimental conditions. The catalyst was recycled in the subsequent run after filtration without any further treatment. Alternatively, the catalyst was regenerated by washing with distilled water before reusing it in the successive run. The recovery of the catalyst was always > 98%. Samples were removed periodically and analyzed by high-performance liquid chromatography with an Alltech OA-10308 column (300 × 7.8 mm) with UV (set at λ = 210 nm) and refractive index detection to analyze the mixture of the samples. An aqueous H₃PO₄ solution (0.1 wt%) was used as the eluent. Products were identified by comparison with the original samples.

Hydrogen peroxide detection and degradation test

A 1 mM solution of H₂O₂ (15 mL) was stirred at the appropriate temperature under a N₂ atmosphere. The pH value of the solution was adjusted by adding Na₂CO₃ (0.5 M, pH 7.5). The amount of the catalyst added was the same as that in the sorbose oxidation (about 200 mg). Hydrogen peroxide was quantified by sampling by permanganate titration. The following procedure has been set up: a sample (5 mL) of the filtered reaction solution was titrated with a 0.01 N KMnO₄ solution at a constant pH value of 7.5 ± 0.1 (by addition of concentrated H₂SO₄). The detection limit of H₂O₂ was 0.01 mM.

Characterization

The metal content and the metal leaching were checked by ICP analysis of the filtrate, on a Jobin Yvon JY24 instrument.

Samples for TEM characterization were prepared by depositing an ethanol suspension of the catalyst onto lacey-carbon-coated 300 mesh copper grids. The particle morphology of the supported nanoparticles, specifically the nanoparticle size, was first investigated by TEM with a Philips LaB6 electron microscope operated at 200 kV and equipped with a Gatan charge-coupled-device camera. Detailed high-resolution HAADF STEM imaging and XEDS analyses were performed with an FEI Titan3 microscope operated at 200 kV accelerating voltage for a deeper investigation of the AuPt-alloy structure of the AuPt/TiO₂ catalyst. This microscope was equipped with double aberration correctors, to provide ultra-high-resolution HAADF STEM images, and an Oxford Inca energy-dispersive X-ray spectrometer equipped with a 30 mm² ultrathin window Si/Li X-ray detector. XEDS data were collected either as spectrum images, in which a focused electron probe was scanned across a region of interest during data collection, or in stationary spot mode, in which an emitted X-ray spectrum from 0–20 keV was acquired from a specific point on a particle with a probe size less than 0.5 nm. Spectra were acquired with a probe current of approximately 0.5 nA and dwell times of between 200 and 400 ms per pixel in the case of maps and 20–30 seconds per analysis in spot mode. STEM digital images were acquired by using the FEI TIA software, and the Oxford Inca microanalysis software was used for XEDS acquisition and analysis. The atomic fractions of gold and platinum were quantified by the Cliff–Lorimer method on relative intensities of the Pt-Lα and Au-Lα peaks with k-factors provided by the XEDS system manufacturer. The AuPt particle size distribution and the total metal dispersion were determined by counting 250 particles in the HAADF STEM images with GAUSS software.

The acid/base properties of the supports were measured with a Metrohm Titrino 718 instrument. Typically, sample (100 mg) was dispersed in a 10⁻³ M KCl solution (50 mL). The mixture was kept overnight at room temperature with vigorous stirring and the pH value of the solution was measured.

Nitrogen adsorption isotherms were measured at T = -196 °C with a TriStar 3000 volumetric adsorption analyzer manufactured by Micromeritics Instrument Corp. (Norcross, GA). Before adsorption measurements, the carbon powders were degassed in flowing nitrogen for 1–2 h at T = 200 °C. The specific surface area of the samples was calculated with the Brunauer–Emmett–Teller method within the relative pressure range of 0.05–0.20.

Keywords: carbohydrates · gold · oxidation · platinum · supported catalysts

- [1] T. Mallat, A. Baiker, *Chem. Rev.* **2004**, *104*, 3037–3058.
- [2] S. E. Davis, M. S. Ide, R. J. Davis, *Green Chem.* **2013**, *15*, 17–45.
- [3] M. Sankar, N. Dimitratos, P. J. Miedziak, P. P. Wells, C. J. Kiely, G. J. Hutchings, *Chem. Soc. Rev.* **2012**, *41*, 8099–8139.
- [4] M. Besson, P. Gallezot, C. Pinel, *Chem. Rev.* **2014**, *114*, 1827–1870.
- [5] A. Villa, N. Dimitratos, C. E. Chan-Thaw, C. Hammond, L. Prati, G. J. Hutchings, *Acc. Chem. Res.* **2015**, *48*, 1403–1412.
- [6] H. Zhang, N. Toshima, *Catal. Sci. Technol.* **2013**, *3*, 268–278.
- [7] C. Brönnimann, Z. Bodnar, P. Hug, T. Mallat, A. Baiker, *J. Catal.* **1994**, *150*, 199–211.
- [8] C. Brönnimann, T. Mallat, A. Baiker, *J. Chem. Soc. Chem. Commun.* **1995**, 1377–1378.
- [9] C. Brönnimann, Z. Bodnar, R. Aeschmann, T. Mallat, A. Baiker, *J. Catal.* **1996**, *161*, 720–729.
- [10] T. Mallat, C. Brönnimann, A. Baiker, *J. Mol. Catal. A* **1997**, *117*, 425–438.
- [11] T. Mallat, C. Brönnimann, A. Baiker, *Appl. Catal. A* **1997**, *149*, 103–112.
- [12] S. N. Sidorov, I. V. Volkov, V. A. Davankov, M. P. Tsyurupa, P. M. Valetsky, L. M. Bronstein, R. Karlinsey, J. W. Zwanziger, V. G. Matveeva, E. M.

- Sulman, N. V. Lakina, E. A. Wilder, R. J. Spontak, *J. Am. Chem. Soc.* **2001**, *123*, 10502–10512.
- [13] L. M. Bronstein, G. Goerigk, M. Kostylev, M. Pink, I. A. Khotina, P. M. Valetsky, V. G. Matveeva, E. M. Sulman, M. G. Sulman, A. V. Bykov, N. V. Lakina, R. J. Spontak, *J. Phys. Chem. B* **2004**, *108*, 18234–18242.
- [14] T. Reichstein, A. Gruessner, *Helv. Chim. Acta* **1934**, *17*, 311–328.
- [15] E. Grünewald, U. Prüße, K.-D. Vorlop, *Catal. Today* **2011**, *173*, 76–80.
- [16] A. Villa, G. M. Veith, L. Prati, *Angew. Chem.* **2010**, *122*, 4601–4604; *Angew. Chem. Int. Ed.* **2010**, *49*, 4499–4502.
- [17] G. L. Brett, Q. He, C. Hammond, P. J. Miedziak, N. Dimitratos, M. Sankar, A. A. Herzing, M. Conte, J. A. Lopez-Sanchez, C. J. Kiely, D. W. Knight, S. H. Taylor, G. J. Hutchings, *Angew. Chem.* **2011**, *123*, 10318–10321; *Angew. Chem. Int. Ed.* **2011**, *50*, 10136–10139.
- [18] A. Villa, S. Campisi, K. M. Mohammed, N. Dimitratos, F. Vindigni, M. Manzoli, W. Jones, M. Bowker, G. J. Hutchings, L. Prati, *Catal. Sci. Technol.* **2015**, *5*, 1126–1132.
- [19] N. Dimitratos, A. Villa, D. Wang, F. Porta, D. Su, L. Prati, *J. Catal.* **2006**, *244*, 113–121.
- [20] L. Prati, A. Villa, *Acc. Chem. Res.* **2014**, *47*, 855–863.
- [21] W. C. Ketchie, Y. Fang, M. S. Wong, M. Murayama, R. J. Davis, *J. Catal.* **2007**, *250*, 94–101.
- [22] L. Prati, P. Spontoni, A. Gaiassi, *Top. Catal.* **2009**, *52*, 288–296.
- [23] M. Sankar, N. Dimitratos, D. W. Knight, A. F. Carley, R. Tiruvalam, C. J. Kiely, D. Thomas, G. J. Hutchings, *ChemSusChem* **2009**, *2*, 1145–1151.

Received: September 4, 2015

Published online on November 27, 2015